

# Simulation of Terahertz Doppler Wavelength Shifting of Infrared Optical Pulses in an Active Semiconductor Layer

Igor V. Scherbatko, Alexander G. Nerukh, *Member, IEEE*, and Stavros Iezekiel, *Member, IEEE*

**Abstract**—In this paper, a time-domain model of wavelength shifting in a semiconductor layer with a constant stimulated gain level and moving Bragg grating of permittivity is used to investigate Doppler conversion of an infrared ( $f_0 = 200$  THz) ultra-short (0.4-ps width) optical pulse. Simulations of the electromagnetic-field evolution show that the high drift velocity of carriers in InGaAsP can produce at least 1-THz conversion span. The optical power of the converted pulse can be as much as 20% of the power in the initial pulse. The backscattered pulses and pulses transmitted through the semiconductor layer depend dramatically on the permittivity modulation depth and length of the layer. It has been demonstrated that the length of the semiconductor layer can be optimized to produce strong converted pulses of short duration.

**Index Terms**—Doppler wavelength shifting, gain, moving Bragg grating, permittivity modulation, semiconductor, time-domain, Volterra integro-differential equation.

## I. INTRODUCTION

ALTHOUGH multigigabit-per-second bit rates are available in single-wavelength optical communications, WDM techniques offer a more effective means of realizing the massive bandwidth potential of optical fiber. A vital component in future high-capacity dynamic WDM systems will be the wavelength converter. Such devices will be used to prevent wavelength blocking at optical cross connects and to increase the capacity and reconfigurability of a network with a fixed set of wavelengths.

Wavelength conversion can be achieved with a number of methods, and an excellent comparison of them has been carried out by Yoo [1]. Techniques for wavelength conversion in fiber-optic links can be classified broadly as either direct electrooptic or all-optical. An electrooptic converter can be easily realized by photodetecting the incoming signal and then retransmitting it using a laser onto a different wavelength, but the need to convert to and from the optical domain leads to complexity and high power consumption. In contrast, all-optical wavelength converters enable direct translation of the information on the incoming wavelength to a new wavelength without

entering the electrical domain [2]. Consequently, most current research is focused on all-optical wavelength conversion in semiconductor optical amplifiers using either cross-gain modulation, cross-phase modulation, or four-wave mixing (FWM).

Cross-gain modulation suffers from limited transparency and signal-to-noise deterioration due to a large spontaneous emission background. Signal quality is further reduced by chirping and amplitude distortion due to carrier modulation [1]. Cross-phase modulation is hampered by the interferometric nature of such wavelength conversion, which restricts the dynamic range of the input power, adds extra difficulty in controlling input power levels, and has limited transparency [1].

Semiconductors injected with high-concentration carriers are suitable materials for nondegenerate four-wave mixing (NDFWM) in the 1.3–1.6- $\mu\text{m}$  wavelength range used in optical communications. Many experiments have been reported on using traveling-wave semiconductor optical amplifiers (TWA's), in which pump and signal beams are coupled externally [3]–[5]. Others have used Fabry–Perot laser diodes (LD's) where the lasing wavelength is injection locked by an external master laser [6]. Both methods need an external laser in addition to a probe source and require careful coupling of the laser beam to the waveguide.

Some investigators are developing new schemes based on hybrid TWA/LD devices. For example, NDFWM in a distributed feedback (DFB) laser appears to be a relatively straightforward approach. NDFWM was demonstrated in a long-cavity  $\lambda/4$ -shifted DFB laser using its lasing beam as a pump [7]. A maximum conversion efficiency of  $-6$  dB at wavelength detuning of 1.75 nm and a conversion range of 6 THz were demonstrated experimentally without the assistance of Fabry–Perot resonance. The long-cavity DFB laser used in the experiments has a three-electrode structure and a bias current of about 400 mA. A similar super structure grating distributed Bragg reflector (DBR) laser has been used for 10-Gb/s signal tunable wavelength conversion over a range of 30 nm [8]. However, all attempts to exclude an external pump-beam source in highly degenerate FWM experiments lead to the use of complicated hybrid DFB(DBR)/TWA optical semiconductor devices. In fact, the NDFWM scheme needs a relatively strong input signal, which, in turn, requires pre-amplification.

In all the above cases, the useful output of the device is a FWM-generated sideband. A common problem is that the wave-mixing products (sidebands) are not easily separated from the pump and/or the probe. Consequently, most FWM schemes use very narrow passband optical filters to isolate the desired

Manuscript received March 15, 1999. The work of I. Scherbatko was supported under a Royal Society/NATO Post-Doctoral Fellowship for joint research with the Institute of Microwaves and Photonics, School of Electronic and Electrical Engineering, The University of Leeds.

I. V. Scherbatko and A. G. Nerukh are with the Technical University of Radio Electronics, Kharkov State University, Kharkov 310726 Kharkov, Ukraine.

S. Iezekiel is with the Institute of Microwaves and Photonics, School of Electronic and Electrical Engineering, The University of Leeds, Leeds, LS2 9JT, U.K.

Publisher Item Identifier S 0018-9480(00)02532-1.

converted signal. To overcome this drawback, a novel class of FWM-based devices has been proposed in which optical filtering is not required [9]. High-efficiency noncollinear FWM in a broad-area TWA has been demonstrated. However, the practicality appears doubtful given the complexity of the two pump arrangement and signal adjustment using beam-shaping optics. A further and common disadvantage of FWM schemes in semiconductor amplifiers is rapidly decreasing conversion efficiency with conversion span.

FWM in TWA's is based on two physical phenomena that occur in a semiconductor medium. Input and pump beams propagate in a semiconductor and interfere. The interference inside the amplifier generates a spatially and temporally modulated carrier density, which produces an index and gain traveling-wave grating. The signal beam deflects from the traveling-wave permittivity grating and its frequency is up or down shifted compared to the initial value.

A question arises as to whether it is possible to generate appropriate spatial and/or temporal permittivity modulation in a semiconductor for continuous wavelength shifting of an input signal by current injection alone, rather than signal interference. Chirping in TWA's is an example of such frequency shifting, where pulse current modulation of the semiconductor medium leads to both amplitude and frequency modulation in the output signal. The existence of the former is unwanted, and the nanosecond pulse modulation of the strong currents involved (hundreds of milliampere) poses difficulties. Moreover, the resulting value of wavelength shifting is inadequate.

Media with time-varying parameters have also been used, with the Doppler effect, to implement wavelength conversion, but at microwave frequencies. Lampe *et al.* [10] have shown, theoretically and experimentally, that when an electromagnetic pulse is incident upon a moving ionization front, the pulse can be simultaneously shifted up in frequency and compressed in duration. For example, this phenomenon produces intense pulses of radiation with a wavelength of 8 mm by reflecting an incident 3.2-cm wavelength microwave pulse off the front of a high-current relativistic electron beam, which plays the role of an overdense plasma. A free-carrier plasma can be generated in semiconductors either by strong current injection or illumination with an external laser pulse. Such an approach has been used for generation of ultrafast mid-infrared laser pulses [11], [12].

A new mechanism of electromagnetic-wave frequency conversion by modulation of the medium permittivity has been recently proposed [13]. In addition, an enhancement of the reflection coefficient at a moving plasma boundary in a waveguide structure has been established. It has been shown that a combination of these two phenomena may result in a qualitatively new effect that consists of an enhancement of the optical frequency shift. Possible applications of these phenomena in a WDM optical transmission systems have been proposed. In [14], an electromagnetic-wave interaction with a plasma cluster moving in a waveguide was analyzed. It is shown that the wavelength shifting of the initial signal can be achieved with amplification. This owes to the presence of a double-dispersion mechanism: plasma and waveguide dispersions.

In this paper, we investigate an alternative approach to wavelength conversion using only the Doppler effect in combination

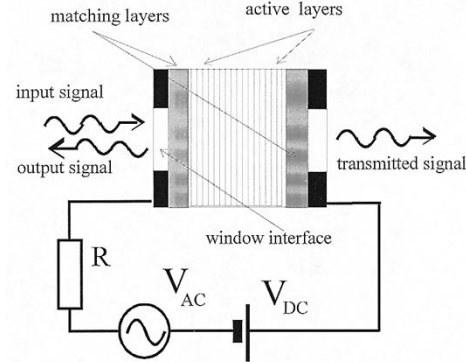


Fig. 1. Proposed Doppler wavelength shifter.

with a semiconductor layer in which a moving Bragg grating of permittivity is excited by an external modulated electric field [15]. In contrast to the FWM scheme, the wavelength conversion technique reported here does not rely on nonlinear properties of the semiconductor medium to implement a moving refractive index grating. Hence, it dispenses with the need for a pump laser, and thereby overcomes the need for polarization control. Furthermore, unlike FWM and cross gain modulation schemes, there is no need to filter out the probe wavelength because the backscattered signal only contains the converted wavelengths, and not the original pre-conversion wavelengths.

The paper is organized as follows. In Section II, we provide a schematic diagram of a prototype device and discuss the model of the semiconductor Doppler shifter. The time-domain integro-differential equation, which describes the evolution of the electromagnetic field in the active semiconductor layer, is described in Section III. Using the estimations of semiconductor layer parameters, the numerical simulations of wavelength shifting are discussed in Section IV.

## II. MODEL FOR SEMICONDUCTOR DOPPLER WAVELENGTH SHIFTER

To obtain Doppler wavelength shifting, a moving grating of semiconductor plasma density should be generated in an active layer. We propose to use strong current injection into a semiconductor layer to create a moving carrier density grating. Since the time and spatial dependent permittivity and conductivity of the semiconductor medium vary with the local carrier density, a traveling refractive index grating is induced.

A prototype device is proposed in Fig. 1, where the active semiconductor layer employs ohmic contacts with a window interface. Carriers injected into the active layer from the negative contact drift toward the positive contact under application of the electric field. The dc voltage is augmented by a modulation from an external microwave oscillator. Strong modulation of the injected current leads to spatial-time modulation of current density and forms the traveling refractive index grating. By choosing a special semiconductor layer structure (e.g., with heterojunction or multiple quantum wells), we obtain a semiconductor gain medium. The proposed Doppler wavelength shifter is similar in structure to surface-emitting semiconductor lasers, but without mirrors.

The strongest reflection of an optical signal is realized by a Bragg grating. If the wavelength of an optical signal in free space is  $\lambda_0$ , the Bragg period should be  $\Lambda = \lambda_0/2n$ , where  $n$  is the refractive index of semiconductor medium. For  $\lambda_0 = 1.5 \mu\text{m}$  and InGaAsP ( $n = 3.6$ ), this yields  $\Lambda = 0.208 \mu\text{m}$ . The electron drift velocity  $v_D$  is proportional to the applied electric field  $E$  as  $v_D = -\mu_n E$ , where  $\mu_n$  is the electron mobility. The electron mobility for different semiconductors varies widely and the maximal  $v_D$  differs for different semiconductors by orders of magnitude, e.g., for GaAs  $v_D = 10^5 \text{ ms}^{-1}$  [16] and for InAs  $v_D = 10^6 \text{ ms}^{-1}$  [17]. If we assume that the maximal drift velocity of electrons in InGaAsP is the same as in GaAs, the current modulation frequency should be  $f_m = v_D/\Lambda \approx 0.5 \text{ THz}$ . Among numerous microwave devices reported to date, the resonant-tunneling diode has demonstrated oscillations of approximately 700 GHz [17]. For such very high frequencies, the microwave oscillator will have to be integrated with the wavelength shifting layer in one device.

The amount of wavelength shift by a moving ionization front in a semiconductor medium for a normally incident optical pulse can be calculated using [10]

$$f_s/f_0 = (1 + \beta)/(1 - \beta)$$

where  $f_0$  and  $f_s$  are the frequencies of the incident and reflected waves, respectively,  $\beta$  is a ratio between  $v_D$  and the velocity of light in a medium:  $\beta = v_D/(c/n)$ . For  $\lambda_0 = 1.5 \mu\text{m}$  ( $f_0 = 200 \text{ THz}$ ) and  $v_D = 10^5 \text{ ms}^{-1}$ ,  $\beta \approx 0.0012$ . Therefore,  $f_s \approx 1.0025 f_0 = 200.48 \text{ THz}$ , which corresponds to a frequency shift of 0.96 THz in absolute value for co- and counter-propagating schemes. Usually, the difference between channels in WDM systems is no more than 100 GHz and a conversion span of about 1 THz allows the multiplexing of at least ten channels. Continuous tuning of the frequency-shifted signal can be achieved by varying of the carrier drift velocity in the external electric field.

The electromagnetic model used in the calculations takes into account the electromagnetic transients of short optical pulses in the gain medium with time and spatial variations in permittivity. Here, moving Bragg gratings of refractive index in a semiconductor are investigated for their suitability to wavelength shift short infrared optical pulses. In particular, attention is focused on a generic shifter structure with a one-dimensional (layered) structure, in which variations in permittivity as a function of both distance and time are accounted for. The influence of propagating optical signals on carrier density (photocurrent phenomenon) is neglected.

The layered structure considered in the following analysis is shown schematically in Fig. 2. The active region is defined by two-plane boundaries separated by a length  $L$  along the longitudinal ( $\xi$ ) axis. The dielectric constant outside the semiconductor layer is  $\varepsilon$ . Here,  $E_o$  is an optical signal that is incident on a semiconductor layer,  $E_s$  is a backscattered electric field (reflected signal), and  $E_p$  is the electric field transmitted through the layer. In order to describe wave propagation in a semiconductor active medium, it is useful to introduce a complex refractive index  $n = n' - jn''$ . The stimulated gain  $g_{st}$  is related to  $n''$  by  $g_{st} = -2kn''$ , where  $k$  denotes the free-space

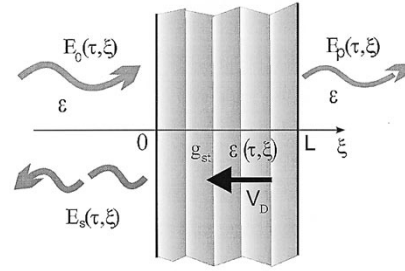


Fig. 2. Model of the semiconductor Doppler wavelength shifter.

wavenumber. Gain coefficients in semiconductors with stimulated emission of the order of several hundreds of  $\text{cm}^{-1}$  yield a  $n''$  of  $-10^{-3}, \dots, -10^{-2}$ , which is a significant quantity. The stimulated emission also affects the real part  $n'$  of the refractive index since  $n'$  and  $n''$  are linked by the Kramers–Krönig relations. In fact,  $n'$  is more strongly affected by the stimulated emission than  $n''$ , which is expressed by a parameter  $\alpha = \delta n'/\delta n''$ , relating a change in  $n''$  to a change in  $n'$ . This  $\alpha$ -parameter is of the order of  $\alpha \approx 3 \dots 7$  [18]. It is assumed that the stimulated gain is uniformly distributed inside the semiconductor layer and  $n'' = -0.007$  ( $g_{st} = 580 \text{ cm}^{-1}$ ). Consideration is given here to the case of the spatial–time distribution of the dielectric constant as a traveling Bragg grating

$$\varepsilon(\tau, \xi) = \varepsilon \left\{ 1 + A \sin [\eta(\beta\tau + \xi)] \right\} \quad (1)$$

where  $\tau$  and  $\xi$  are normalized time and spatial coordinates, respectively,  $A$  is the amplitude of the permittivity modulation (contrast factor), and  $\eta$  is a normalized frequency.

Let  $\beta = 0.0012$ ; this denotes the relative velocity of the modulated Bragg grating in the reflected medium. The directions of the grating and incident signal are opposing. The parameter  $A$  can be estimated using the relationship between the refractive index variation in an InAs semiconductor. This has been done by Visser and Blok [19]. In their research,  $\delta n \approx 0.1$ , resulting in  $(\varepsilon + \delta\varepsilon)/\varepsilon = ((n + \delta n)/n)^2 \approx 1 + (2\delta n/n)$  or  $\varepsilon + \delta\varepsilon \approx \varepsilon(1 + (2\delta n)/n)$ . For this case,  $(2\delta n)/n \approx 0.05$ , therefore, we can set  $A = 0.025$ . To solve this transient electromagnetic problem, an integro-differential equation approach is used.

### III. TIME-DOMAIN INTEGRO-DIFFERENTIAL EQUATION

The principal component of the electromagnetic model used in the present calculations is the time-domain integro-differential equation. To build a model of a nonstationary electromagnetic process in a semiconductor medium, we assume that such a medium can be described by a permittivity  $\varepsilon$  and conductivity  $\sigma$ . Suppose that  $\bar{E}_0(t, \bar{r})$  is an initial electric field that was in existence for  $t < 0$  in the medium whose permittivity was  $\varepsilon$  and conductivity was zero. Beginning at time  $t = 0$ , the permittivity and the conductivity is determined by the function  $\varepsilon_1(t)$  and  $\sigma(t)$ , respectively. The relative permeability is equal to one. For

$t \geq 0$ , the electric field intensity then satisfies the integro-differential Volterra equation of the second kind [20]

$$\bar{E}(t, \bar{r}) = \bar{E}_0(t, \bar{r}) + \int_0^\infty dt' \int_\infty dr' \left\{ \langle \bar{x} | \Gamma_e | \bar{x}' \rangle \frac{\varepsilon_1(t') - \varepsilon}{\varepsilon} + \langle \bar{x} | \Gamma_j | \bar{x}' \rangle \mu_0 \sigma(t') \right\} \cdot \bar{E}(t', \bar{r}') \quad (2)$$

where

$$\langle \bar{x} | \Gamma_e | \bar{x}' \rangle = \frac{1}{4\pi} \left( \nabla \nabla - \frac{1}{v^2} \frac{\partial^2}{\partial t^2} \right) \frac{\delta(t - t' - \frac{1}{v} |\bar{r} - \bar{r}'|)}{|\bar{r} - \bar{r}'|} \quad (3)$$

$$\langle \bar{x} | \Gamma_j | \bar{x}' \rangle = \frac{v^2}{4\pi} \left( \nabla \nabla - \frac{1}{v^2} \frac{\partial^2}{\partial t^2} \right) \frac{\theta(t - t' - \frac{1}{v} |\bar{r} - \bar{r}'|)}{|\bar{r} - \bar{r}'|}. \quad (4)$$

The velocity of light in the initial medium is  $v = c/\sqrt{\varepsilon}$ , where  $c$  is the velocity of light in free space,  $\mu_0$  is the magnetic permittivity in *vacuo*,  $\nabla$  is the nabla operator,  $\delta(t)$  is the Dirac delta function,  $\theta(t)$  is the Heaviside unit function, and  $\bar{x} = (t, \bar{r})$ .

For the unidirectional case, we can assume that all values depend on the single spatial coordinate  $x$ , and the vectors have components perpendicular to the  $x$  axis. After integrating over transverse coordinates in (2), we then have the following scalar integro-differential equation:

$$E(t, x) = E_0(t, x) - \frac{1}{2\varepsilon v} \int_0^\infty dt' \times \int_{-\infty}^\infty dx' \left\{ \left( \varepsilon_1(t') - \varepsilon \right) \frac{\partial}{\partial t'} + \frac{\sigma(t)}{\varepsilon_0} \right\} \times \delta\left(t - t' - \frac{1}{v} |x - x'| \right) E(t', x'). \quad (5)$$

We can switch to normalized variables in (5) by setting  $\tau = vkt$  and  $\xi = kx$ , where  $k$  is a scaling factor with the wavenumber dimension, which yields

$$\bar{E}(\tau, \xi) = \bar{E}_0(\tau, \xi) - \frac{1}{2} \int_0^\infty d\tau' \times \int_{-\infty}^\infty d\xi' \left\{ b(\tau') + \frac{1 - a^2(\tau', \xi)}{a^2(\tau', \xi)} \frac{\partial}{\partial \tau} \right\} \times \delta(\tau - \tau' - |\xi - \xi'|) E(\tau', \xi') \quad (6)$$

where

$$b(\tau) = \frac{\sigma\left(\frac{\tau}{vk}\right)}{\varepsilon \varepsilon_0 v k} \\ a^2(\tau, \xi) = \frac{\varepsilon}{\varepsilon_1\left(\frac{\tau}{vk}\right)} \\ \bar{E}(\tau, \xi) = E\left(\frac{\tau}{vk}, \frac{\xi}{k}\right).$$

The parameters  $a$  and  $b$  are linked with the real and imaginary parts of the refractive index as  $a^2 = \varepsilon/(n'^2 - n''^2)$ ,  $b = (\eta/\varepsilon)n'n''$ .

Since the electric field exhibits jumps when the medium parameter changes abruptly, it is appropriate to consider the elec-

tric flux density  $D(\tau, \xi) = \varepsilon(\tau/vk)\bar{E}(\tau, \xi)$ , which remains continuous. Using the equation

$$\delta(\tau - \tau' - |\xi - \xi'|) = \delta(\xi' - \xi - \tau + \tau') + \delta(\xi' - \xi + \tau - \tau')$$

from (6), we get the integro-differential equation for the electric flux density

$$D(\tau, \xi) = \frac{1}{a^2(\tau, \xi)} D_0(\tau, \xi) - \frac{1}{2} \frac{\partial}{\partial \tau} \times \int_0^\tau d\tau' \frac{a^2(\tau', \xi)}{a^2(\tau, \xi)} \left\{ b(\tau', \xi) + \frac{1 - a^2(\tau', \xi)}{a^2(\tau', \xi)} \frac{\partial}{\partial \tau} \right\} \times [D(\tau', \xi + \tau - \tau') + D(\tau', \xi - \tau + \tau')] \quad (7)$$

where  $D_0(\tau, \xi) = \varepsilon \bar{E}_0(\tau, \xi)$ . Transition to differentiation with respect to the variable  $\xi$  in (7) yields the starting equation for further numerical calculation

$$D(\tau, \xi) = D_0(\tau, \xi) - \frac{1}{2} \frac{\partial}{\partial \xi} \int_0^\tau d\tau' (1 - a^2(\tau', \xi)) \times [D(\tau', \xi + \tau - \tau') + D(\tau', \xi - \tau + \tau')] - \frac{1}{2} \int_0^\tau d\tau' b(\tau') a^2(\tau', \xi) [D(\tau', \xi + \tau - \tau') + D(\tau', \xi - \tau + \tau')]. \quad (8)$$

For the numerical solution of (8), we assume a uniform grid on the coordinate plane  $(\tau, \xi)$  with equal time  $\Delta\tau$  and spatial  $\Delta\xi$  steps  $\Delta\tau = \Delta\xi$ . This equality meets the stability condition for the numerical analysis  $\Delta x \leq v\Delta t$ . The integration paths in (8) are then straight diagonal lines, which pass through nodes of the grid. The essence of the proposed methodology is the sequential solution of (8) by marching in time step by step, as described in [20].

#### IV. NUMERICAL EXAMPLES

The numerical investigations were carried out for the propagation of a square 0.4-ps width TEM optical pulse with initial frequency  $f_0 = 200$  THz through the semiconductor layer with stimulated gain and permittivity modulated as a moving Bragg grating. With normalized coordinates, the incident signal has the form of a rectangular traveling pulse with a sinusoidal subcarrier and unity magnitude

$$E_0(\tau, \xi) = \frac{1}{\pi} \left\{ \arctan(-50[\tau - \xi - 50]) + \arctan(50[\tau - \xi - 1]) \right\} \cos(10(\tau - \xi)).$$

For the initial moment  $\tau = 0$ , the front of the pulse is located near the first layer's boundary. The variation of permittivity in the active layer is given by

$$\varepsilon(\tau, \xi) = 3.5 \{1 + A \sin[20(0.0012\tau + \xi)]\}.$$

To demonstrate the above method, we calculate the reflected ( $E_s$ ) and transmitted ( $E_p$ ) fields, which are the result of

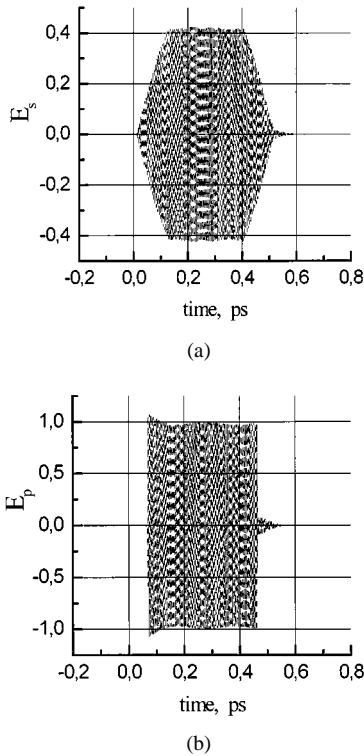


Fig. 3. (a) Dependence of backscattered electric field on time for  $L = 5 \mu\text{m}$  and  $A = 0.025$ . (b) Dependence of passed electric field on time for  $L = 5 \mu\text{m}$  and  $A = 0.025$ .

backscattering and amplification of the initial field. We obtain the field distribution in time by solving (8) for selected spatial coordinates ( $\xi = -1$  for the backscattered field and  $\xi = L$  for the field transmitted through the layer). A numerical solution is obtained through discretization in space and time, with an integration time step of  $1/40$  of the oscillation period being used throughout this study.

Consideration is first given to the electromagnetic-field evolution in a short ( $L = 5 \mu\text{m}$ ) semiconductor layer with a permittivity modulation depth 2.5% ( $A = 0.025$ ). Fig. 3(a) shows the magnitude of the reflected signal versus time. The resulting backscattered pulse is slightly greater than 0.4 ps in width and has a trapeziform envelope. The peak magnitude of the backscattered signal does not exceed 40% of the initial signal. The pulse that is transmitted through the semiconductor layer is shown in Fig. 3(b). Since the layer is not long enough for strong amplification of the initial signal to occur, the magnitude of the transmitted field does not differ greatly from the initial value. The spectral densities of the initial, backscattered, and transmitted signals are shown in Fig. 4. As expected, the maximum value of the spectrum power of the reflected signal (curve 2) corresponds to a frequency of 200.5 THz.

It is convenient to define the normalized optical power as  $|E|^2$  and investigate the envelope evolution of signals. Fig. 5 shows that if the coefficient  $A$  is set to 0.0125, the backscattered pulse magnifies its peak power and width, when the length of the layer increases from 5 to 25  $\mu\text{m}$ . Note that for the last curve ( $L = 25 \mu\text{m}$ ), the reflected pulse consists of two short peaks and the second pulse has even greater magnitude than the first. The propagation time of the pulse through the active layer in this

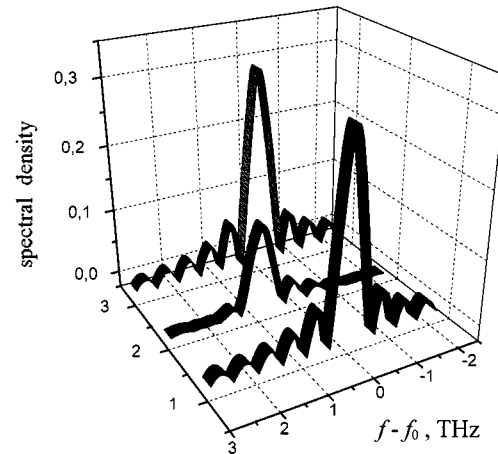


Fig. 4. Spectral densities of (1—initial signal, 2—reflected signal, 3—passed signal) for  $L = 5 \mu\text{m}$  and  $A = 0.025$ .

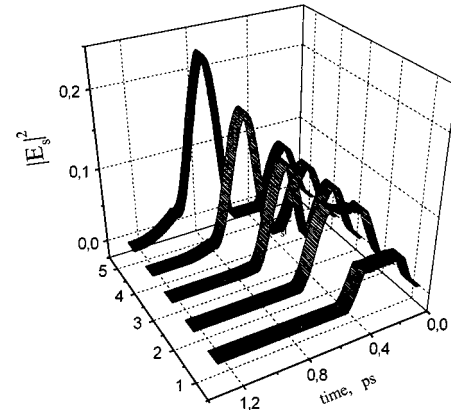


Fig. 5. Envelopes of the reflected optical power for  $A = 0.0125$  and length of semiconductor layer (1—5  $\mu\text{m}$ , 2—10  $\mu\text{m}$ , 3—15  $\mu\text{m}$ , 4—20  $\mu\text{m}$ , 5—25  $\mu\text{m}$ ).

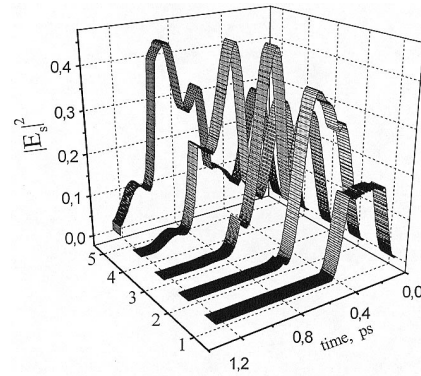


Fig. 6. Envelopes of the reflected optical power for  $A = 0.025$  and length of semiconductor layer (1—5  $\mu\text{m}$ , 2—10  $\mu\text{m}$ , 3—15  $\mu\text{m}$ , 4—20  $\mu\text{m}$ , 5—25  $\mu\text{m}$ ).

case is comparable with the pulse duration of  $t_{\text{prop}} = (L/c)n \approx 0.3 \text{ ps}$ . This leads to the superimposing of resonance oscillations (in the layer with gain) on the external signal and the layer then emits back secondary optical pulses containing significant optical power.

In Fig. 6, it is shown that when the permittivity modulation depth is set to twice the previous value ( $A = 0.025$ ) there is, as anticipated, an increase in the peak power of backscattered

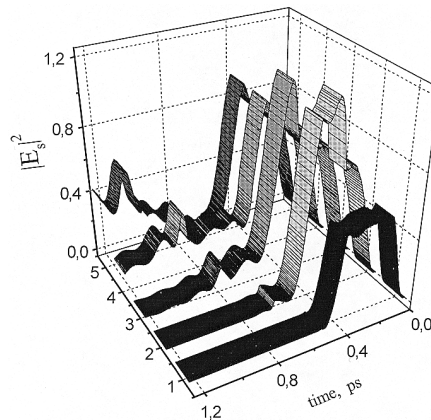


Fig. 7. Envelopes of the reflected optical power for  $A = 0.05$  and length of semiconductor layer (1—5  $\mu\text{m}$ , 2—10  $\mu\text{m}$ , 3—15  $\mu\text{m}$ , 4—20  $\mu\text{m}$ , 5—25  $\mu\text{m}$ ).

pulses. However, it is seen that when the length of the semiconductor layer is more than 15  $\mu\text{m}$ , the reflected pulses' envelopes are strongly corrupted by resonance oscillations.

If a moving Bragg grating with higher contrast is used, then a more powerful output signal is obtained. When the permittivity modulation depth is 5% ( $A = 0.05$ ), the best reflected pulses are generated if the length of the layer is no more than 10  $\mu\text{m}$ . The envelope of the reflected pulse for  $L = 10 \mu\text{m}$  is also modulated by a resonant frequency, but the damping rate is sufficiently high for this not to be problematic. This phenomenon is shown in Fig. 7. After reaching the saturation level in power  $|E_s|^2 = 1.2$  for the 10- $\mu\text{m}$  length of layer, the peak power then decreases to 0.9. In this case, the reflected signal does not vanish at the period of calculations. The appearance of continuous oscillations may give rise to unacceptable pulse-detection errors. The transition to continuous oscillation for the transmitted optical signal is clearly shown in Fig. 8(a). Note that the electromagnetic transients in the active layer lead to the appearance of two strong peaks. Between these peaks (during the time from 0.3 to 0.7 ps) there is a stabilization period where the optical power of the input signal is distributed between the reflected and transmitted signals. After the second peak, the transmitted signal takes on the form of continuous oscillations. These oscillations are analogous to lasing in a semiconductor laser. The optical signal transmitted through the semiconductor layer ( $E_p$ ) for  $A = 0.05$  and  $L = 25 \mu\text{m}$  has the same frequency as the initial one. Its spectral density is shown in Fig. 8(b) as a dashed line, while the spectrum of the reflected signal is shown here as a solid line. Since resonance oscillations dramatically disturb the backscattered signal's envelope, the spectral density of the output pulse has strongly asymmetrical characteristics.

The wavelength conversion efficiency is defined as the ratio between the maximum value of the output signal power to the input power. Note that a permittivity modulation depth of 5% and a stimulated gain level of  $g_{st} = 580 \text{ cm}^{-1}$  for a 10- $\mu\text{m}$ -long active semiconductor layer is enough to realize a conversion efficiency of 0.8 dB.

The above results imply that, for a permittivity modulation depth of 2%–5%, the main portion of reflections occurs in the initial 5–10  $\mu\text{m}$  of the active semiconductor medium. In practice, the width of the converted pulse is a very important pa-

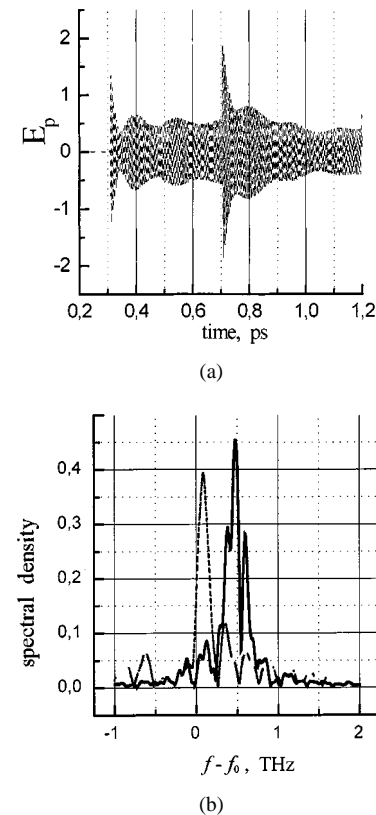


Fig. 8. (a) Dependence of passed electric field on time for  $A = 0.05$  and  $L = 25 \mu\text{m}$ . (b) Spectral densities of the reflected optical pulse (solid line) and passed signal (dashed line) for  $A = 0.05$  and  $L = 25 \mu\text{m}$ . Spectral densities of the reflected optical pulse (solid line) and passed signal (dashed line) for  $A = 0.05$  and  $L = 25 \mu\text{m}$ .

rameter and should be as short as possible. The latter is essentially determined by the gain, coefficient  $A$ , and length of the active layer. It is clear from the above simulations that for  $A = 0.025$ –0.05 and  $g_{st} = 580 \text{ cm}^{-1}$ , the length of the semiconductor layer should be no more than 10  $\mu\text{m}$ . This provides a further advantage over schemes that use optical amplifiers since such devices are typically 1-mm long and require currents of the order of 500 mA. Since the proposed scheme uses a significantly shorter length of active semiconductor, its power consumption should be significantly less.

## V. CONCLUSION

An active semiconductor layer whose stimulated gain and permittivity were modulated as a moving Bragg grating was investigated for optical frequency conversion. A time-domain model was used to study a Doppler wavelength conversion of an infrared  $f_0 = 200 \text{ THz}$  ( $\lambda_0 = 1.5 \mu\text{m}$ ) 0.4-ps width optical pulse. In order to calculate the ultrafast electromagnetic transients, a time-domain Volterra integro-differential equation was used. It was shown that the high-drift velocity of carriers in an InGaAsP semiconductor can produce at least 1-THz conversion span. The converted pulsewidth and spectral density depend strongly on the changes in permittivity modulation, with the modulation depth having to be at least 2%–5%. A conversion efficiency of 0.8 dB can be obtained for a stimulated gain of  $g_{st} = 580 \text{ cm}^{-1}$ , modulation depth of about 5%, and a

semiconductor layer of 10- $\mu\text{m}$  length. It has been demonstrated that, owing to resonance oscillations in the semiconductor layer with gain, the envelope of the reflected pulse can be corrupted dramatically and the signal transmitted through the layer can become quasi-continuous.

The proposed method has significant advantages compared to existing wavelength converters that are based on semiconductor optical amplifiers. Firstly, it removes the requirement for a probe laser, and with it, the need to maintain polarization control between pump and probe signals. Secondly, it does not need to use a nonlinear medium to generate the moving Bragg grating. Moreover, the backscattered signal does not contain components from the probe signal and, hence, there is no need for optical filtering as in FWM and cross gain modulation schemes. Finally, the relatively short lengths of semiconductor layers needed to realize sufficient Doppler shifts will lead to reduced power consumption compared to semiconductor optical amplifier wavelength converters.

## REFERENCES

- [1] S. J. B. Yoo, "Wavelength conversion technologies for WDM network applications," *J. Lightwave Technol.*, vol. 14, pp. 955–965, June 1996.
- [2] T. Durhuus, B. Mikkelsen, C. Joergensen, S. L. Danielsen, and K. E. Stubkjaer, "All-optical wavelength conversion by semiconductor optical amplifiers," *J. Lightwave Technol.*, vol. 14, pp. 942–953, June 1996.
- [3] S. Scotti, E. Iannone, A. Mecozzi, A. D'Ottavi, and P. Spano, "Efficiency of frequency translators based on four-wave mixing in semiconductor optical amplifiers," *Pure Appl. Opt.*, vol. 4, pp. 385–389, 1995.
- [4] A. D'Ottavi, F. Martelli, P. Spano, A. Mecozzi, S. Scotti, R. Dall'Ara, J. Eckner, and G. Guekos, "Very high efficiency four-wave mixing in a single semiconductor traveling-wave amplifier," *Appl. Phys. Lett.*, vol. 68, pp. 2186–2188, 1996.
- [5] A. Uskov, J. Mork, J. Mark, M. C. Tatham, and G. Sherlock, "THz four-wave mixing in semiconductor optical amplifiers," *Appl. Phys. Lett.*, vol. 65, pp. 944–946, 1994.
- [6] E. Cerbonechi, D. Hennequin, and E. Arimondo, "Frequency conversion in external cavity semiconductor lasers exposed to optical injection," *IEEE J. Quantum Electron.*, vol. 32, pp. 192–200, 1996.
- [7] H. Kuwatsuka, H. Shoji, M. Matsuda, and H. Ishikawa, "Nondegenerate four-wave mixing in a long-cavity  $\lambda/4$ -shifted DFB laser using its lasing beam as a pump beams," *IEEE J. Quantum Electron.*, vol. 33, pp. 2002–2010, Nov. 1997.
- [8] H. Yasaka *et al.*, "Finely tunable 10-Gb/s signal wavelength conversion from 1530- to 1560-nm region using a super structure grating distributed Bragg reflector laser," *IEEE Photon. Technol. Lett.*, vol. 8, pp. 764–766, June 1996.
- [9] D. X. Zhu, S. Dubovitsky, W. H. Steier, K. Uppal, D. Tishinin, J. Burger, and P. D. Dapkus, "Noncollinear four-wave mixing in a broad area semiconductor optical amplifier," *Appl. Phys. Lett.*, vol. 70, no. 16, pp. 2082–2084, Apr. 1997.
- [10] M. Lampe, E. Ott, and J. H. Walker, "Interaction of electromagnetic waves with a moving ionization front," *Phys. Fluids*, vol. 21, no. 1, pp. 42–54, Jan. 1978.
- [11] J. Meyer and A. Y. Elezzabi, "Subpicosecond reflection switching of 10  $\mu\text{m}$  radiation using semiconductor surfaces," *Appl. Phys. Lett.*, vol. 58, pp. 1940–1943, May 1991.
- [12] A. Y. Elezzabi and J. Meyer, "Simulation of the generation of ultrafast midinfrared laser pulses," *IEEE J. Quantum Electron.*, vol. 28, pp. 1830–1834, Aug. 1992.
- [13] A. Nerukh, I. Scherbatko, and M. Marciniak, "Electromagnetic wave frequency shift by temporal variation of medium parameters," *Pr. Inst. Lacznosci.*, no. 110, pp. 7–27, 1998.
- [14] A. Nerukh and N. Khizhnyak, "Enhanced reflection of an electromagnetic wave from a plasma cluster moving in a waveguide," *Microwave Opt. Technol. Lett.*, vol. 17, no. 4, pp. 267–273, 1998.
- [15] I. V. Scherbatko, A. G. Nerukh, and S. Iezekiel, "Terahertz double-Doppler wavelength shifting of infrared optical pulses in excited semiconductor medium," in *IEEE 6th Int. Terahertz Electron. Conf.*, Leeds, U.K., Sept. 1998, pp. 211–214.
- [16] T. Merlet, D. Dolfi, and J. P. Huignard, "A traveling fringes photodetector for microwave signals," *IEEE J. Quantum Electron.*, vol. 32, pp. 778–782, May 1996.
- [17] E. R. Brown, J. R. Soderstrom, C. D. Parker, L. J. Mahoney, K. M. Molvar, and T. C. McGill, "Oscillations up to 712 GHz in InGa/AlSb resonant-tunneling diodes," *Appl. Phys. Lett.*, vol. 58, no. 20, pp. 2291–2293, May 1991.
- [18] K. Petermann, "Laser diode modulation and noise," in *Advances in Optoelectronics*. Norwell, MA: Kluwer, 1988, vol. 3, p. 315.
- [19] T. D. Visser, H. Blok, and D. Lenstra, "Modal analysis of a planar waveguide with gain and losses," *IEEE J. Quantum Electron.*, vol. 31, pp. 1803–1810, Oct. 1995.
- [20] A. G. Nerukh, I. Scherbatko, and O. Rybin, "The direct numerical calculation of an integral Volterra equation for an electromagnetic signal in a time-varying dissipative medium," *J. Electromag. Waves Applicat.*, vol. 12, pp. 163–173, 1998.



**Igor V. Scherbatko** received the M.S. degree in electronics, the M.S. degree in mathematics, and the Ph.D. degree in physics and electronics from the Kharkov Technical University of Radio and Electronics (KhTURE), Kharkov, Ukraine, in 1988, 1993, and 1994, respectively.

From 1988 to 1994, he was a Senior Engineer in the Electronics Department, KhTURE, where he took part in the industrial program of research and development of microwave fiber-optic systems. His specific research was concentrated on the simulation of heterolasers. From 1994 to 1996, he was an Assistant Professor in the Department of High Mathematics, KhTURE. Since 1996, he has been an Associate Professor at KhTURE. In 1998, he was with the Engineering and Electronics Department, Technical University of Berlin, as Visiting Researcher. He is currently a Research Fellow at the Institute of Microwave and Photonics, The University of Leeds, Leeds, U.K. His current research interests include the time-domain numerical simulation of optoelectronic devices, electromagnetic propagation through a complex medium, and electromagnetic transients. He has published over 30 publications and holds one patent.

Dr. Scherbatko was the recipient of a Deutscher Akademischer Austauschdienst Scholarship.

**Alexander G. Nerukh** (M'96) was born in the Sumy region, Ukraine, in 1944. He received the Diploma radiophysics degrees, Candidate of Sciences degree (Ph.D.) in radiophysics, and the Doctor of Science in radiophysics from the Kharkov State University, Kharkov, Ukraine, in 1968, 1975, and 1991, respectively.

He was involved in research projects dealing with ionosphere investigations by virtue of incoherent scattering of radio waves, and then studied the problem of applications of integral equations of electrodynamics in describing electromagnetic wave interactions with moving media and their boundaries. From 1974 to 1977, he was a Research Worker in the Radioholography Laboratory, Kharkov State University. In 1977, he was an Associated Professor in the Department of Higher Mathematics, Kharkov Institute of Radioelectronics (now the Kharkov Technical University of Radioelectronics). In 1991, he became a Professor. He is currently the Head of the Department of Higher Mathematics. During this same period, he followed the development of an integral-equation method in macroscopic electrodynamics, in part in electrodynamics of nonstationary media whose properties and boundaries change in time. His main scientific interests are in electrodynamics, field theory, radiophysics, mathematical physics, and complex function theory. He has published over 70 papers, and authored *Modern Problems of Transient Macroscopic Electrodynamics* (1991). He was recommended by the American Biographical Institute Inc. for biographical inclusion in the American Biographical Institute's *Sixth Edition of the International Directory of Distinguished Leadership* (1996).

Dr. Nerukh is a member of an organizing committee member of the Trans Black Sea Region Scientific Union of Applied Electromagnetism (BSUAE). He had been an active member of the New York Academy of Sciences. He was the recipient of a 1993 grant presented by the International Soros Foundation, the International Soros Science Education Program of the International Renaissance Foundation.



**Stavros Iezekiel** (S'88–M'90) was born in Coventry, U.K., in 1966. He received the B.Eng. and Ph.D. degrees from The University of Leeds, Leeds, U.K., in 1987 and 1991, respectively.

From 1991 to 1993, he worked in conjunction with the M/A-COM Corporate R&D Center on the development of microwave photonic multichip modules. Since 1993, he has been a Lecturer in high-frequency analog electronics at The University of Leeds, Leeds, U.K. His microwave photonics research activities include high-speed semiconductor LD's and lightwave

network analysis techniques.

Dr. Iezekiel is a member of the UKRI MTT-S/ED/AP-S/LEOS Joint Chapter AdCom and is also the membership development officer for the IEEE UKRI Section. He was a co-recipient of the 1999 Institution of Electrical Engineer (IEE) Measurement Prize for his work on lightwave network analysis.